Carbon Nano-Sphere Derived From Crop Residues by Acidic Lithium Bromide Treatment and as an Excellent Adsorbent to Both Heavy Ions and Methyl Orange

Jian Chen
Qilu University of Technology
Xianqin Lu (lxq_sdu@163.com)
Qilu University of Technology
Bingbing Li
Shandong Shunfeng Biological Technology Co□LTD
Cuihua Dong
Qilu University of Technology
Wenyuan Zhu
Nanjing Forestry University

Research Article

Keywords: corn stover, carbon spheres, acidic LiBr, Cr(VI), methyl orange

Posted Date: March 22nd, 2021

DOI: https://doi.org/10.21203/rs.3.rs-309508/v1

Abstract

Carbon spheres, as a widely used carbon material, has attracted extensive attentions. The hydrothermal carbonization (HTC) method was a promising candidate for production of carbon-sphere. But the raw lignocellulose was natural resistant and hardly transformed into the carbon-spheres during HTC. Herein, acidic lithium bromide (LiBr) was supplied in the HTC process to break the resistance of lignocellulose and promoted the nano-carbon spheres forming in mild conditions: 140°C for 150 min. The carbon spheres from raw corn stover showed decent morphology properties and abundant functional groups, which was better than that from pine and poplar wood. It led to the high removal efficiency of the biochar-corn stover to both heavy ions and methyl orange in the waste water. Meanwhile, the filtrate under the optimal reaction was already reused. After five runs, the recycling showed slight effect on the morphology properties and the adsorption capability of biochar. These results verified the practical production of biochar spheres from lignocellulose in mild conditions, which provided more potential for the synthesis of novel biomass-based materials for wide applications.

1 Introduction

Biochar is a carbon-rich material formed by heating biomass under certain conditions(Ahmad et al., 2014). The biochar have excellent application prospects in environmental remediation with the advantages of abundant feedstocks, specific surface area, abundant functional groups, microporosity, and ion exchange capacity (Wang & Wang, 2019a). As a friendly environmental adsorbent, biochar showed adsorption capability to the metal ions and aromatic compounds, such as hexavalent chromium, iron ions, and methyl violet, polycyclic aromatic hydrocarbons and chlorobenzene(Qiu et al., 2009; Vithanage et al., 2017; Zhang et al., 2019a; Zhang et al., 2018). Currently biochar has received more and more attentions, and many researches were performed to improve the properties of biochar.

The fabrication of carbon spheres has attracted extensive attention in the field of materials science. Due to its unique properties, such as surface functional chemical groups, surface area and controllable particle size, carbon spheres have broad application prospects in catalysis, electrochemical conversion, energy storage and environmental purifications (Bai et al., 2018; Liang et al., 2008; Mao et al., 2018; Mi et al., 2008; Siyasukh et al., 2018; Tian et al., 2019). The properties of carbon spheres were highly relied on the synthesis method. Over the past decades, many researchers made great efforts on the synthesis methods of carbon spheres, such as the template methods (hard template and soft template), the hydrothermal carbonization method and the microemulsion polymerization method (Fechler et al., 2013; Mao et al., 2018; Mi et al., 2008). Template methods involved multi-steps: a) the synthesis of the template, b) the preparation of the carbon precursors, c) the pyrolysis carbonization process, d) template removal in a harsh condition (Claesson & Philipse, 2005). The complex coating process and the harsh post-treatment condition of hard template method restricted its wide applications (Tian et al., 2019). The soft template methods omitted the harsh post-treatment process, but it raised high demands for the templates. Many soft template precursors were employed with emulsion droplets, micelles or surfactant as templates, which could be decomposed during carbonization process(Fechler et al., 2013). In soft

template methods, the template should tolerate the temperature before the carbonization and decompose during the carbonization process (Liang et al., 2008). In addition, the high tendency of carbon precursors to crosslinking resulted in the challenge to forming monodispersed carbon spheres (Liu et al., 2015). Compared with template methods, the hydrothermal carbonization method (HTC) has many advantages, such as environmental friendliness and mild treatment condition. The hydrothermal carbonization methods were commonly performed at temperature from 200°C to 250°C for about 12 h to 48 h (Sevilla & Fuertes, 2009; Simsir et al., 2017). Many biomass derived carbon precursors could be transformed to spherical carbon through the HTC methods, such as glucose, fructose and sucrose (Mao et al., 2018; Mi et al., 2008; Nizamuddin et al., 2017; Tian et al., 2019). However, the raw lignocellulose was resistant to hydrothermal treatment and hardly produced the carbon spheres during HTC process (Simsir et al., 2017), (Zhang et al., 2019b). The acidic concentrated lithium bromide hydrolysis(ALBH)process was reported as a green and recyclable method to break the resistant of biomass and cleave the linkage between cellulose to glucose under mild conditions without any pretreatment (80°C-110 ℃) (Lu et al., 2020), (Pan & Li, 2015; Yang et al., 2016). Thus, the ALBH method was performed in this study to break the resistance of raw biomass and further transform to carbon sphere by increasing the severity of heat treatment.

The biochar synthesis depended on the synthesis biomass types and conditions (Li et al., 2017). The raw lignocellulose, such as agricultural residues and forest waste, was abundant in nature, which was the most common feedstock for biochar synthesis (Zhang et al., 2015). The properties of lignocellulose such as the compositions of carbon precursor, the inorganic compounds, the degree of crystalline etc., were reported to effect the properties of biochar (Zhang et al., 2015). In addition, many researches showed that the parameters of synthesis conditions, such as temperature, rate of heating, and residence time et al., also effected the properties of biochar (Nizamuddin et al., 2017; Zhang et al., 2015). Thus, this study was performed to prepare biochar by using different biomass as raw materials under the ALBH method. As well as, by operating various parameters, the optimum condition to yield carbon nano-spheres was determined. The properties of prepared biochar has been analyzed by scanning electron microscope (SEM), Fourier transform infrared spectroscopy (FTIR), Brunauer-Emmett-Teller (BET) etc.. As well as, the adsorption capacity of biochar to heavy metal ions (Cr(VI)) and polyvalent aromatic hydrocarbons (methyl orange, MO) were also detected.

2 Materials And Methods

2.1 Materials

Poplar and pine chips were provided by Shandong Sun Paper United Co., Ltd (Jining, China) and corn stover were obtained from farmland in Jinan, Shandong Province. Lithium bromide was in reagent grade purchased from Macklin Reagent Co., Ltd. Holocellulose was prepared from corn stover as reported by Guo et al.(Guo et al., 2014). Lignin was provided by Shandong Longlive Bio-Techology Co., Ltd. (China).

2.2 Preparation of biochar

The preparation of biochar was carried out in a closed high temperature reactor as describe before(Lu et al., 2020; Lu et al., 2019). In briefly, the feedstocks were reacted with 60 wt% lithium bromide and 0.5 M HCl at 140°C for 150 min. After the reaction, the carbon residue and the filtrate were separated by suction filtration. The filtrate was collected and stored at 4°C. The solid residue was washed with the tap water to neutrality, and it was dried in an oven at 40°C for 24 h.

The yields of biochar prepared by ALBH method were calculated using the following formula:

$$Biochar\ \ yield\ \ \% = \ \left(\frac{amount\ of\ carbon\ residue\ after\ ALBH(\mathrm{g})}{initial\ amont\ of\ feedstock(\mathrm{g})}\right)\ \times 100\ \ \%$$

2.3 Characterization of biochar

The Fourier transform infrared spectroscopy (FTIR) of biochar were performed using infrared spectrometer (ALPHA, BRUKER, Germany) to analyze its surface functional groups. The element composition was analyzed by X-ray photoelectron spectroscopy (XPS). The Brunauer-Emmett-Teller (BET) surface of biochar was measured by the automatic gas adsorption analyzer ASAP 2460 (micromeritics, USA). The morphology and structure of biochar were analyzed by Hitachi regulus 8220 (Japan) scanning electron microscope (SEM).

2.4 Adsorption experiments

265 mg/L Cr (VI) concentration solution were prepared by dissolving $K_2Cr_2O_7$ into distilled water (made by Qilu University of Technology). The pH of the solution was adjusted by HCl. 0.05 g biochar and 25 mL Cr (VI) solution were incubated at 150 rpm, 37°C for 24 h in an automatic thermostatic oscillator. After incubation, the residue and supernatant were separated by filtration. The concentration of Cr(VI) in the supernatant was measured by UV-visible spectrophotometer at 540 nm as reported before(Lu et al., 2019).

The concentrated methyl orange solution (500 mg/L) was prepared by dosage of methyl orange in distilled water were prepared, and the pH of the solution was adjusted to 2 with HCl. Then 400 mg/L, 200 mg/L, 100 mg/L, 50 mg/L, and 10 mg/L Cr(VI) concentration gradient was carried out by diluted the concentrated solution with HCl aqueous (pH 2). The removal ratio of biochar to methyl orange was carried out by mixing 0.1 g biochar and 10 mL methyl orange solution. The adsorption was performed by shaking the mixture in an automatic thermostatic oscillator at 150 rpm, 37°C for 24 h. After that, the residue and solution were filtered, and the concentration of methyl orange was detected by UV-visible spectrophotometer at 470 nm as described before(Siyasukh et al., 2018).

3. Results And Discussion

3.1 The production and characterization of biochar from lignocellulose by ALBH

In this study, poplar, pine and corn stover were selected as carbon precursor to produce biochar with ALBH treatment. Vaughn et al. reported that the composition of carbon precursor was an essential factor influencing the production of biochar (Vaughn et al., 2013). Lignocellulose as the carbon precursor, cellulose, hemicellulose and lignin are the main components. The chemical composition of pine was analyzed as 41.2 % cellulose, 18.1 % hemicellulose, and 27.3 % lignin. Poplar was composed of 42.9 % cellulose, 24.3 % hemicellulose, and 24.2 % lignin. And that for corn straw was 32.6 % cellulose, 13.9 % hemicellulose and 17.1 % lignin (Lu et al., 2016). It reported that the linkage of hemicellulose was easily cleaved with thermal treatment, and cellulose could endure relatively high temperature with decomposition temperature from 315°C to 400°C during pyrolysis process (van Zandvoort et al., 2013; Zhang et al., 2015). Lignin, aromatic polymer in nature, was reported to be thermally stable (Ragauskas et al., 2014; van Zandvoort et al., 2013).

Table 1 showed the elemental composition of biochar produced from corn stover, pine and poplar. The carbon content of biochar prepared from pine wood was 64.49 wt%, that for poplar was 63.46 wt%, and that for corn stover as 61.81 wt%. It suggested that the carbonization was carried outed during the ALBH treatment and biochar was formed from lignocellulose (Kołodyńska et al., 2012; Wang & Wang, 2019a). The yield of biochar was affected by the biomass types, in which 46.71 wt% of biochar yielded from pine, 47.63 wt% biochar was produced with poplar, and that was 40.44 wt% for corn stover. Because of the thermal stability of lignin, high lignin content of pine (27.3 %) and poplar (24.2 %) may be the reason for the high yield of biochar.

Table 1
Element analysis of biochar produced from corn stover, pine and poplar respectively (%)

	Mesh number	C	H	O	N
Corn stover	> 60	61.11	4.76	23.00	4.76
	40–60	61.81	4.87	25.17	4.87
	20–40	62.85	4.59	26.78	4.59
Pine	40–60	64.49	4.83	28.27	4.83
Poplar	40–60	63.46	4.93	29.84	4.93

Figure 1 showed the morphology of biochar, in which the obvious carbon sphere structure was formed, especially for the biochar prepared from corn stover (Fig. 1-a, b, c). It presented uniform and dispersed for the carbon sphere-cron stover. For the biochar prepared from wood pine (Fig. 1-d) and poplar (Fig. 1-e), only few carbon spheres were observed on the biochar surface, and those carbon spheres were cross-linked together. Due to the more resistance structure of pine and poplar, the incomplete carbonization

may lead to the irregular morphology of carbon (Simsir et al., 2017). The BET analysis also confirmed the results as showed in Table 2. The biochar prepared from corn stover obtained 83.89 m^2/g surface area, and poor surface area was observed for the the biochar-pine (42.85 m^2/g) and biochar-poplar (45.80 m^2/g).

Figure 2 showed the functional groups on the surface of biochar was analyzed by FTIR. It suggested that no obvious difference was existed for the chemical groups types in biochars (Fig. 2- a), in which the wide peaks of 2900 cm^{-1} and 3400 cm^{-1} indicate the possible existence of O-H vibration, the partial peaks of 1000 cm^{-1}-1600 cm^{-1} indicate the existence of -C-O and -C = O vibration, and the peaks of about 700 cm^{-1} indicate the existence of -C-H vibration. The FTIR analysis suggested that a large number of hydroxyl and carboxyl oxygen-containing groups were presented on the surface of ALBH biochar (Lu et al., 2020). Wu et al. reported that the oxygen functional groups on the biochar, such as hydroxy, carbonyl, ester and ketone groups, could provide the interaction sites for the removal of metal ions (Wu et al., 2019).

3.2 the forming of nanosphere from lignocellulose during ALBH

It reported that during hydrothermal carbonization process, the lignocellulose would be firstly hydrolyzed to oligomers and glucose, and that was further dehydration to furans and then condensed and polymerized to carbon particles (García-Bordejé et al., 2017; Mi et al., 2008; Sevilla & Fuertes, 2009). In the carbonization, high temperature and long residual time was need. As reported by Hamza et al. nanospheres were obtained from glucose upon 200 ℃ for 48 h, and cellulose (as the carbon precursor) resulted in a lower degree carbonization because of the less degradation(Sevilla & Fuertes, 2009). Because of the natural resistance of lignocellulose, hydrothermal carbonization was hardly processed with lignocellulose. Acidic concentrated LiBr hydrolysis was reported in many researches on the dissolubility and hydrolysis ability to lignocellulose (Deng et al., 2015; Hou et al., 2017; Li et al., 2016; Mosier et al., 2005; Pan & Li, 2015). Recently, Li et al. reported that the cleavage of ethers and demethylation of lignin during acidic concentrated LiBr (Li et al., 2020). From those reports it is possible to construct the process of the formation of carbon nanosphere from lignocellulose during acidic LiBr treatment. That was schematically illustrated in Graphical abstract. Firstly, the cellulose from lignocellulose was able to be dissolved, and part of lignin particles was cleaved from lignin surface in the LiBr solution. At this stage, the LiBr made an important role (Wang & Wang, 2019b). With the present of hydronium ions, the dissolved cellulose was completely conversed to glucose, which could be occurred at mild conditions as reported by Pan et al.(Pan & Li, 2015). Then, the yield of sugars was further carbonized to form carbon spheres as HTC process. In briefly, with the heat treatment, subsequent reactions were occurred from the glucose to form fructose, furfural like compounds, acids and phenols respectively (Sevilla & Fuertes, 2009). By the intermolecular hydration or condensation reaction, soluble polymers from glucose were formed. At the meantime, the polymers were aromatized and the aromatic nuclei were formed. The various species presented in the solution diffused to the surface of the aromatic

nuclei and linked to the nuclei by the oxygen functionalities. As a result of growth process, the carbon spheres were formed and a high concentration of reactive oxygen groups were distributed on the surface of the carbon spheres. From that, the aromatic nuclei was essential for the spheres forming. The self-assembling lignin particles in the solution could provide more hydrophobic spheres core for the growth process. As well as, because of the cleavage of β-O-4 linkages more active -OH was showed on the surface of core providing more linkage. Thus, the cleavage ability of ALBH to cellulose and lignin was favored the forming carbon spheres, in which carbon spheres was formed similar as HTCs.

To verify the mechanism of formation of carbon nanospheres, homocellulose (cellulose and hemicellulose), lignin, and homocellulose-lignin mixture (2:1 w/w) were respectively used as the precursor to produce biochar by same treatment condition, as showed in Fig. 3. It suggested that carbon nano-spheres were formed from homocellulose with irregular diameters from 50 nm to 100 nm (Simsir et al., 2017). With the lignin as the only substrate, some spheres and microporous morphology were observed on the surface of lignin, in which the part of linkage between lignin was cleaved, the hydrophobic lignin link was self-assembled and colloid spheres were formed (~ 100 nm diameter) in the aqueous phase (Lai et al., 2014). From that, the colloid spheres were formed and released from the surface of lignin, and the porous structure of lignin were observed. In the homocellulose-lignin mixture system, the carbon-particles with 100–200 nm diameter were produced, which showed a similar carbon-particles morphology with lignocellulose. Lignin was the main restriction during the hydrolysis of biomass. As described above, corn stover obtained lower content of lignin than that of pine and poplar, which led to the relatively poor yield of production, however, the lower content of lignin in corn stover was in favor to the decomposition of cellulose to glucose. Without pretreatment, glucose was easily produced with corn stover and was further dehydrated to form carbon nano-spheres. As carbon precursor, corn stover performed better than pine and poplar, and it was more available and costless in China. Thus, the production of carbon spheres-corn stover was discussed following.

3.3 The production of carbon spheres from corn stover

The effect of substrate size on the carbon spheres formation was analyzed. The various sized feedstock was prepared as 20 mesh (> 830 μm), 20–40 mesh (380–830 μm) and 40–60 mesh (250–380 μm) sized corn stover. Figure 1a-c showed that carbon spheres could be formed in three sized corn stover. By reducing the feedstock size, the carbon sphere surface appeared rupture and crosslinkage among spheres were being strengthened. The large-sized spheres have been formed for the biochar prepared from the corn stover sized in mesh number less than 60. It indicated that too small particles might not favor the preparation of biochar. The surface area confirmed the results, in which the poor surface area was detected for the biochar from the corn stover in size less than 60 mesh number (< 250 μm), showed in Table 2. It also found that less oxygen function groups were distributed on the surface of biochar prepared from the corn stover with less size, as showed in Fig. 2b. By comparison, the biochar from 20–40 mesh sized corn stalks (380–830 μm) was elected to further study.

Table 2
Surface area of biochar from corn stover, poplar and poplar by BET analysis

Feedstock	Corn stover			Pine	Poplar
Mesh number	20–40	40–60	> 60	40–60	40–60
Surface Area (m^2/g)	75.53	83.89	63.84	42.85	45.80

Table 3 showed the different reaction conditions used to synthesize ALBH biochar from corn stover, as treatment 1 to treatment 7 (T1-T7). The surface morphology of biochar prepared under T1-T7 reactions was observed by SEM showed in Fig. 4. It showed that the carbon spheres on the surface of the biochar are distributed more uniformly under the conditions of T1 (140°C) and T4 (200°C), the particle size of the carbon spheres is severely dispersed under the conditions of T2 (160°C) and T3 (180°C). Under the condition of T4, some of the carbon spheres are cross-linked. The effect of various acid concentration (as T5, T6, T7) on the ALBH reaction was further explored at 140°C. Figure 4b showed that the acid conditions showed slightly effect on the morphology of the biochar. By comparison, the carbon spheres under the condition of 0.8 M acid concentration (T6) showed more uniform morphology. From that, the carbon spheres could be formed and showed well properties under low temperature 140°C for 150 min with 0.8 M of HCl from 20–40 meshed corn stover.

Table 3
The different reaction conditions used to synthesize ALBH biochar from corn stover, as treatment 1 to treatment 7 (T1-T7).

Test	T1	T2	T3	T4	T5	T6	T7
Solid loading (%)	5	5	5	5	5	5	5
Acid (M)	0.5	0.5	0.5	0.5	0.6	0.8	1.0
Time (min)	150	150	150	150	150	150	150
Temperature (°C)	140	160	180	200	140	140	140

3.4 the recyclability of the LiBr solutions

After reaction, the biochar was separated from the reaction system by filtering, and the solution were analyzed by HPLC. No sugar compounds were detected in the filtrate from T6 treatment (20–40 meshed corn stover treated by 140°C for 150 min, 0.8 M HCl). It reported that the production of glucose could be dehydrated and decarboxylated to form furans or humins in high HTC treatment severity (Lu et al., 2020; Lu et al., 2019; Pan & Li, 2015). The dehydration production of sugars, such as 5-hydroxymethylfurfural (5-HMF), furfural and levulinic acid (LA) were detected with an ultraviolet spectrophotometer at 285 nm, in which only slight LA was detected in the filtrate, and almost no 5-HMF and furfural were detected. During the ALBH treatment in this study, the saccharides were mainly reacted to form humins with slight furans. Li et al. reported that lignin and products from lignin were distributed as solid (Deng et al., 2015; Li et al., 2016). Thus, the filtrate after treatment may be reused directly.

Fig. 5 showed the morphology of the biochar prepared from the LiBr solutions with fifth runs recycling, in which carbon spheres with uniform size was observed. The filtrate recovered after the reaction was reused and the biochar was formed and obtained desired yield as 36 %-40 % (40 % for run 1, 38 % for run 2, 38 % for run 3, 38 % for run 4 and 36 % for run 5). The biochar obtained abundant functional groups on the surface for the biochar prepared by the five recycling, showed in Fig. 6. The results verified the recyclability of the treated solution and it confirmed the practical use of ALBH method to produce biochar in commercial applications.

3.5 the removal ability of biochar to heavy ions and methyl orange

Currently, biochar as the adsorbent was usually used in the removal of heavy ions and organic chemicals in environmental remediation(Bai et al., 2018; Dai et al., 2020; Kazakis et al., 2018; Zhao et al., 2017). The Cr(VI), as one of the most toxic metal ion, could cause many diseases, such as dermatitis and lung cancer, highly threating human health (Gao & Xia, 2011; Kazakis et al., 2018). But Cr(VI) was wildly used in industrial areas, including leather, electroplating, wood preservation, petroleum refining (Gao & Xia, 2011). The biochar as an adsorbent showed efficiency in the removal ions of the waste water. The agriculture residues such as the corn cob, the rice husk and apple peels were used as feedstock to produce biochar. But as reported before, the biochar produced from pyrolysis corn cob with $ZnCl_2$ and NH_4Cl only obtained 34.48 mg/g theoretical maximum adsorption ability to Cr(VI) at 45°C (Tang et al., 2016). 25.02 mg/g maximum adsorption capacity to Cr(VI) was got by the biochar produced from rice husk heated at 700°C with NaOH for 5 h got. (B.D. Mukri, 2016). As well as the biochar was pyrolyzed from apple peels with the adsorption capacity of 36.01 mg/g to Cr(VI) (Enniya et al., 2018). Lu et al., used to reported that the adsorption of elephant grass-ALBH biochar obtained maximum adsorption capability of 99.43 mg/g biochar(Lu et al., 2020). Table 4 showed the adsorption capability of biochar to hexavalent chromium (Cr(VI)) with 265 mg/L initial Cr(VI) concentration. The biochar with corn stover treated in T6 condition obtained 110.99 mg/g adsorption capability to Cr(VI). It suggested that the removal ratio of corn stover-ALBH biochar was high than the elephant grass-ALBH biochar in this study. And the recycling showed slight effect on the adsorption capability of biochar to heavy ions, in which 94.71 mg/g adsorption ability was obtained after fiive recycling runs. As an adsorbent, the surface area and the functional groups played an important role in the interaction between the ions and the biochar. In this study, the morphology spheres provided more binding sites for the ions, meanwhile, the abundant functional groups also improved the adsorption of biochar to heavy ions.

Table 4
The adsorption capacity of biochar to Cr(VI) during five runs of continual recycling of LiBr solution

Runs		**1**	**2**	**3**	**4**	**5**
Adsorption capacity (mg/g)	110.99	105.01	104.98	103.13	95.09	94.71

Figure 7 showed the removal ratio of biochar for methyl orange. Methyl orange as a water-soluble azo dye is widely used in the industrial. The adsorption was an effective technology used for methyl orange removal due to the low cost, simple preparation technique, easy to recycle. Herein, the corn stover-ALBH biochar got high potential in the removal methyl orange than many reported carbon spheres (Siyasukh et al., 2018). It indicated that a well linear correlation was detected between the concentration of methyl orange and the adsorption capability of biochar, in which the adsorption capability of biochar to methyl orange was increased with the initial dosage of methyl orange. With the further increase of the dosage of methyl orange to 2000 mg/ g biochar, 84.81 % removal ratio was obtained to methyl orange.

4 Conclusions

As a green and recyclable strategy, LiBr treatment could one-pot transform raw corn stover to carbon spheres. That carbon spheres showed decent morphology properties and abundant functional groups, which was better than that from pine and poplar wood. By optimizing the reaction conditions, a stable spherical structure was obtained and it showed strong removal capacity to both heavy metal ions and methyl orange. And the recycling of the LiBr solution was verified. These results confirmed its strong application potential in biomass utilization.

Declarations

Declaration of Competing Interest

The authors declare that they have no known competing financial interests or personal relationships that could have appeared to influence the work reported in this paper.

Acknowledgements

This study was financially supported by the Foundation of State Key Laboratory of Biobased Material and Green Papermaking (No.2419010205, No. 23190444 and KF201823), The foundation of the Jiangsu Provincial Key Laboratory of Pulp and Paper Science and Technology (No. KL201906), Natural Science Foundation of Shandong Province (ZR2019BC022), and National Natural Science Foundation of China (Grant No. 31901269).

References

1. Ahmad, M., Rajapaksha, A.U., Lim, J.E., Zhang, M., Bolan, N., Mohan, D., Vithanage, M., Lee, S.S., Ok, Y.S. 2014. Biochar as a sorbent for contaminant management in soil and water: a review. *Chemosphere*, **99**, 19-33.
2. B.D. Mukri, K.K., A. Chowdhury, D. Suryakala, C. Subrahmanyam,. 2016. Alkali-treated carbonized rice husk for the removal of aqueous Cr(VI). *Bioresources*, **11**(4), 9175–9189.

3. Bai, J., Huang, Y., Gong, Q., Liu, X., Li, Y., Gan, J., Zhao, M., Shao, Y., Zhuang, D., Liang, J. 2018. Preparation of porous carbon nanotube/carbon composite spheres and their adsorption properties. *Carbon*, **137**, 493-501.
4. Claesson, E.M., Philipse, A.P. 2005. Monodisperse magnetizable composite silica spheres with tunable dipolar interactions. *Langmuir : the ACS journal of surfaces and colloids*, **21**(21), 9412-9419.
5. Dai, L., Wang, Y., Zou, X., Chen, Z., Liu, H., Ni, Y. 2020. Ultrasensitive Physical, Bio, and Chemical Sensors Derived from 1-, 2-, and 3-D Nanocellulosic Materials. *Small*, **16**(13), 1906567.
6. Deng, W., Kennedy, J.R., Tsilomelekis, G., Zheng, W., Nikolakis, V. 2015. Cellulose Hydrolysis in Acidified LiBr Molten Salt Hydrate Media. *Industrial & Engineering Chemistry Research*, **54**(19), 5226-5236.
7. Enniya, I., Rghioui, L., Jourani, A. 2018. Adsorption of hexavalent chromium in aqueous solution on activated carbon prepared from apple peels. *Sustainable Chemistry and Pharmacy*, **7**, 9-16.
8. Fechler, N., Fellinger, T.P., Antonietti, M. 2013. "Salt templating": a simple and sustainable pathway toward highly porous functional carbons from ionic liquids. *Adv Mater*, **25**(1), 75-9.
9. Gao, Y., Xia, J. 2011. Chromium contamination accident in China: viewing environment policy of China. *Environ Sci Technol*, **45**(1520-5851 (Electronic)).
10. García-Bordejé, E., Pires, E., Fraile, J.M. 2017. Parametric study of the hydrothermal carbonization of cellulose and effect of acidic conditions. *Carbon*, **123**, 421-432.
11. Guo, F., Shi, W., Sun, W., Li, X., Wang, F., Zhao, J., Qu, Y. 2014. Differences in the adsorption of enzymes onto lignins from diverse types of lignocellulosic biomass and the underlying mechanism. *Biotechnology for Biofuels*, **7**, 38-38.
12. Hou, Q., Ju, M., Li, W., Liu, L., Chen, Y., Yang, Q. 2017. Pretreatment of Lignocellulosic Biomass with Ionic Liquids and Ionic Liquid-Based Solvent Systems. *Molecules*, **22**(3).
13. Kazakis, N., Kantiranis, N., Kalaitzidou, K., Kaprara, E., Mitrakas, M., Frei, R., Vargemezis, G., Vogiatzis, D., Zouboulis, A., Filippidis, A. 2018. Environmentally available hexavalent chromium in soils and sediments impacted by dispersed fly ash in Sarigkiol basin (Northern Greece). *Environmental Pollution*, **235**, 632-641.
14. Kołodyńska, D., Wnętrzak, R., Leahy, J.J., Hayes, M.H.B., Kwapiński, W., Hubicki, Z. 2012. Kinetic and adsorptive characterization of biochar in metal ions removal. *Chemical Engineering Journal*, **197**, 295-305.
15. Lai, C., Tu, M., Shi, Z., Zheng, K., Olmos, L.G., Yu, S. 2014. Contrasting effects of hardwood and softwood organosolv lignins on enzymatic hydrolysis of lignocellulose. *Bioresour Technol*, **163**, 320-7.
16. Li, H., Dong, X., da Silva, E.B., de Oliveira, L.M., Chen, Y., Ma, L.Q. 2017. Mechanisms of metal sorption by biochars: Biochar characteristics and modifications. *Chemosphere*, **178**, 466-478.
17. Li, N., Pan, X., Alexander, J. 2016. A facile and fast method for quantitating lignin in lignocellulosic biomass using acidic lithium bromide trihydrate (ALBTH). *Green Chemistry*, **18**(19), 5367-5376.

18. Li, Z., Sutandar, E., Goihl, T., Zhang, X., Pan, X. 2020. Cleavage of ethers and demethylation of lignin in acidic concentrated lithium bromide (ACLB) solution. *Green Chemistry*, **22**(22), 7989-8001.
19. Liang, C., Li, Z., Dai, S. 2008. Mesoporous carbon materials: synthesis and modification. *Angewandte Chemie (International ed. in English)*, **47**(20), 3696-3717.
20. Liu, J., Wickramaratne, N.P., Qiao, S.Z., Jaroniec, M. 2015. Molecular-based design and emerging applications of nanoporous carbon spheres. *Nature Materials*, **14**(8), 763-774.
21. Lu, X., Chen, J., Lu, J., Wang, S., Xia, T. 2020. Monosaccharides and carbon nanosphere obtained by acidic concentrated LiBr treatment of raw crop residues via optimizing the synthesis process. *Bioresour Technol*, **310**, 123522.
22. Lu, X., Liu, X., Zhang, W., Wang, X., Wang, S., Xia, T. 2019. The residue from the acidic concentrated lithium bromide treated crop residue as biochar to remove Cr (VI). *Bioresource Technology*, 122348.
23. Lu, X., Zheng, X., Li, X., Zhao, J. 2016. Adsorption and mechanism of cellulase enzymes onto lignin isolated from corn stover pretreated with liquid hot water. *Biotechnol Biofuels*, **9**, 118.
24. Mao, H., Chen, X., Huang, R., Chen, M., Yang, R., Lan, P., Zhou, M., Zhang, F., Yang, Y., Zhou, X. 2018. Fast preparation of carbon spheres from enzymatic hydrolysis lignin: Effects of hydrothermal carbonization conditions. *Sci Rep*, **8**(1), 9501.
25. Mi, Y., Hu, W., Dan, Y., Liu, Y. 2008. Synthesis of carbon micro-spheres by a glucose hydrothermal method. *Materials Letters*, **62**(8-9), 1194-1196.
26. Mosier, N., Wyman, C., Dale, B., Elander, R., Lee, Y.Y., Holtzapple, M., Ladisch, M. 2005. Features of promising technologies for pretreatment of lignocellulosic biomass. *Bioresour Technol*, **96**(6), 673-86.
27. Nizamuddin, S., Baloch, H.A., Griffin, G.J., Mubarak, N.M., Bhutto, A.W., Abro, R., Mazari, S.A., Ali, B.S. 2017. An overview of effect of process parameters on hydrothermal carbonization of biomass. *Renewable and Sustainable Energy Reviews*, **73**, 1289-1299.
28. Pan, X., Li, S. 2015. Saccharification of lignocellulosic biomass. *United States Patent*.
29. Qiu, Y., Zheng, Z., Zhou, Z., Sheng, G.D. 2009. Effectiveness and mechanisms of dye adsorption on a straw-based biochar. *Bioresource Technology*, **100**(21), 5348-5351.
30. Ragauskas, A.J., Beckham, G.T., Biddy, M.J., Chandra, R., Chen, F., Davis, M.F., Davison, B.H., Dixon, R.A., Gilna, P., Keller, M., Langan, P., Naskar, A.K., Saddler, J.N., Tschaplinski, T.J., Tuskan, G.A., Wyman, C.E. 2014. Lignin valorization: improving lignin processing in the biorefinery. *Science*, **344**(6185), 1246843.
31. Sevilla, M., Fuertes, A.B. 2009. The production of carbon materials by hydrothermal carbonization of cellulose. *Carbon*, **47**(9), 2281-2289.
32. Simsir, H., Eltugral, N., Karagoz, S. 2017. Hydrothermal carbonization for the preparation of hydrochars from glucose, cellulose, chitin, chitosan and wood chips via low-temperature and their characterization. *Bioresour Technol*, **246**, 82-87.

33. Siyasukh, A., Chimupala, Y., Tonanon, N. 2018. Preparation of magnetic hierarchical porous carbon spheres with graphitic features for high methyl orange adsorption capacity. *Carbon*, **134**, 207-221.
34. Tang, S., Chen, Y., Xie, R., Jiang, W., Jiang, Y. 2016. Preparation of activated carbon from corn cob and its adsorption behavior on Cr(VI) removal. *Water Science and Technology*, **73**(11), 2654-2661.
35. Tian, H., Liang, J., Liu, J. 2019. Nanoengineering Carbon Spheres as Nanoreactors for Sustainable Energy Applications. *Adv Mater*, e1903886.
36. van Zandvoort, I., Wang, Y., Rasrendra, C.B., van Eck, E.R., Bruijnincx, P.C., Heeres, H.J., Weckhuysen, B.M. 2013. Formation, molecular structure, and morphology of humins in biomass conversion: influence of feedstock and processing conditions. *ChemSusChem*, **6**(9), 1745-58.
37. Vaughn, S.F., Kenar, J.A., Thompson, A.R., Peterson, S.C. 2013. Comparison of biochars derived from wood pellets and pelletized wheat straw as replacements for peat in potting substrates. *Industrial Crops and Products*, **51**, 437-443.
38. Vithanage, M., Herath, I., Joseph, S., Bundschuh, J., Bolan, N., Ok, Y.S., Kirkham, M.B., Rinklebe, J. 2017. Interaction of arsenic with biochar in soil and water: A critical review. *Carbon*, **113**, 219-230.
39. Wang, J., Wang, S. 2019a. Preparation, modification and environmental application of biochar: A review. *Journal of Cleaner Production*, **227**, 1002-1022.
40. Wang, M., Wang, F. 2019b. Catalytic Scissoring of Lignin into Aryl Monomers. *Adv Mater*, **31**(50), e1901866.
41. Wu, J., Wang, T., Zhang, Y., Pan, W.P. 2019. The distribution of Pb(II)/Cd(II) adsorption mechanisms on biochars from aqueous solution: Considering the increased oxygen functional groups by HCl treatment. *Bioresour Technol*, **291**, 121859.
42. Yang, X., Li, N., Lin, X., Pan, X., Zhou, Y. 2016. Selective Cleavage of the Aryl Ether Bonds in Lignin for Depolymerization by Acidic Lithium Bromide Molten Salt Hydrate under Mild Conditions. *J Agric Food Chem*, **64**(44), 8379-8387.
43. Zhang, J., Shao, J., Jin, Q., Li, Z., Chen, H. 2019a. Sludge-based biochar activation to enhance Pb(II) adsorption. *Fuel*, **252**, 101-108.
44. Zhang, K., Sun, P., Faye, M.C.A.S., Zhang, Y. 2018. Characterization of biochar derived from rice husks and its potential in chlorobenzene degradation. *Carbon*, **130**, 730-740.
45. Zhang, X., Hewetson, B.B., Mosier, N.S. 2015. Kinetics of Maleic Acid and Aluminum Chloride Catalyzed Dehydration and Degradation of Glucose. *Energy & Fuels*, **29**(4), 2387-2393.
46. Zhang, X., Zhang, P., Yuan, X., Li, Y., Han, L. 2019b. Effect of pyrolysis temperature and correlation analysis on the yield and physicochemical properties of crop residue biochar. *Bioresour Technol*, **296**, 122318.
47. Zhao, N., Zhao, C., Lv, Y., Zhang, W., Du, Y., Hao, Z., Zhang, J. 2017. Adsorption and coadsorption mechanisms of Cr(VI) and organic contaminants on H3PO4 treated biochar. *Chemosphere*, **186**, 422-429.

Figures

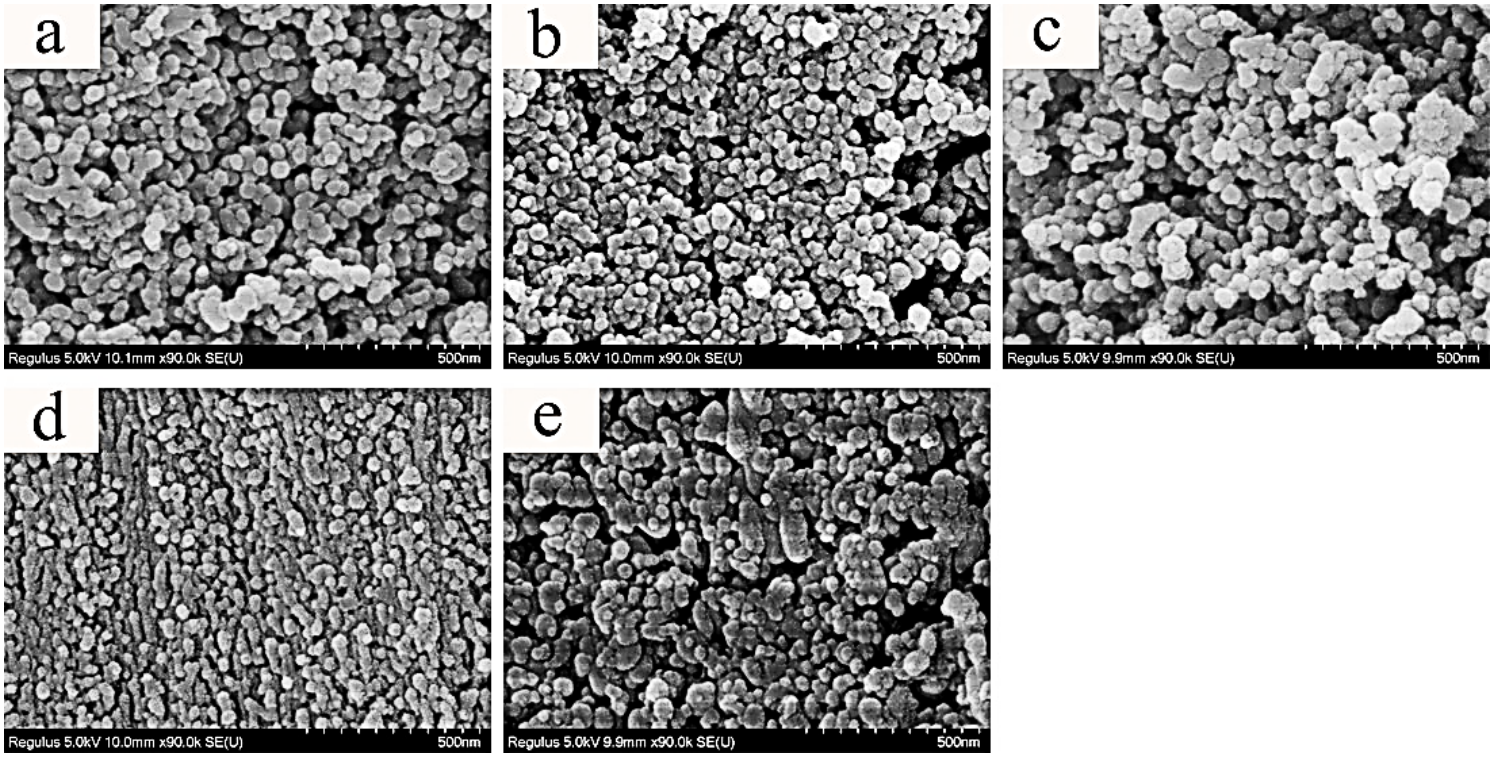

Figure 1

The morphology of biochar produced from corn stover (a-c), pine wood (d) and poplar wood (e) with LiBr treatment. (a-c) means the biochar-corn stover with different feedstock sizes, including 20-40 meshed corn stover (a), 40-60 meshed corn stover (b) and >60 meshed corn stover (c).

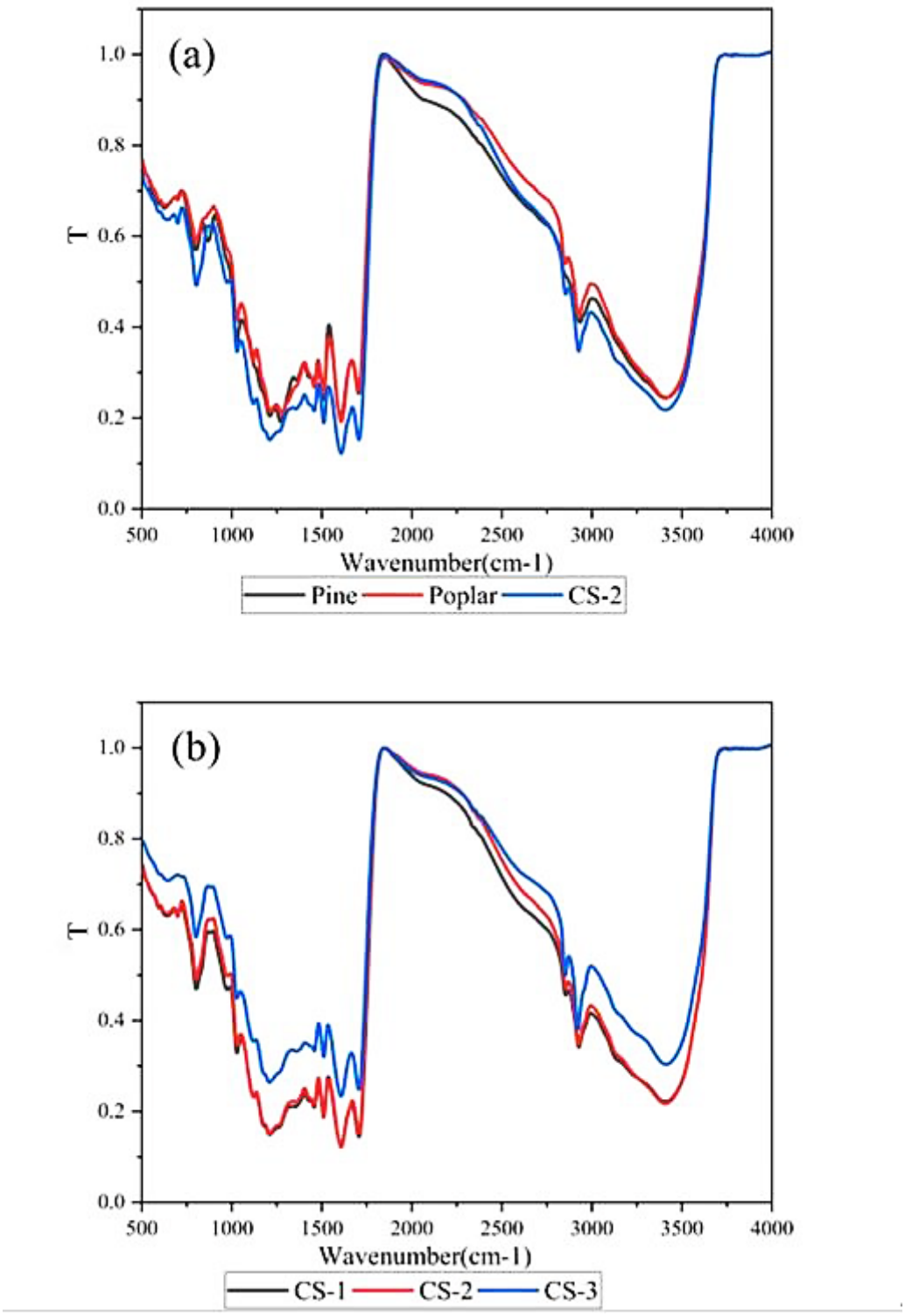

Figure 2

The functional groups presented on the surface of biochar by FTIR. a: the biochar prepared from corn stover, pine and poplar. b: the biochar produced from corn stover with different sizes, including 20-40 meshed corn stalk (CS-1), 40-60 meshed corn stover (CS-2) and >60 meshed corn stalk (CS-3).

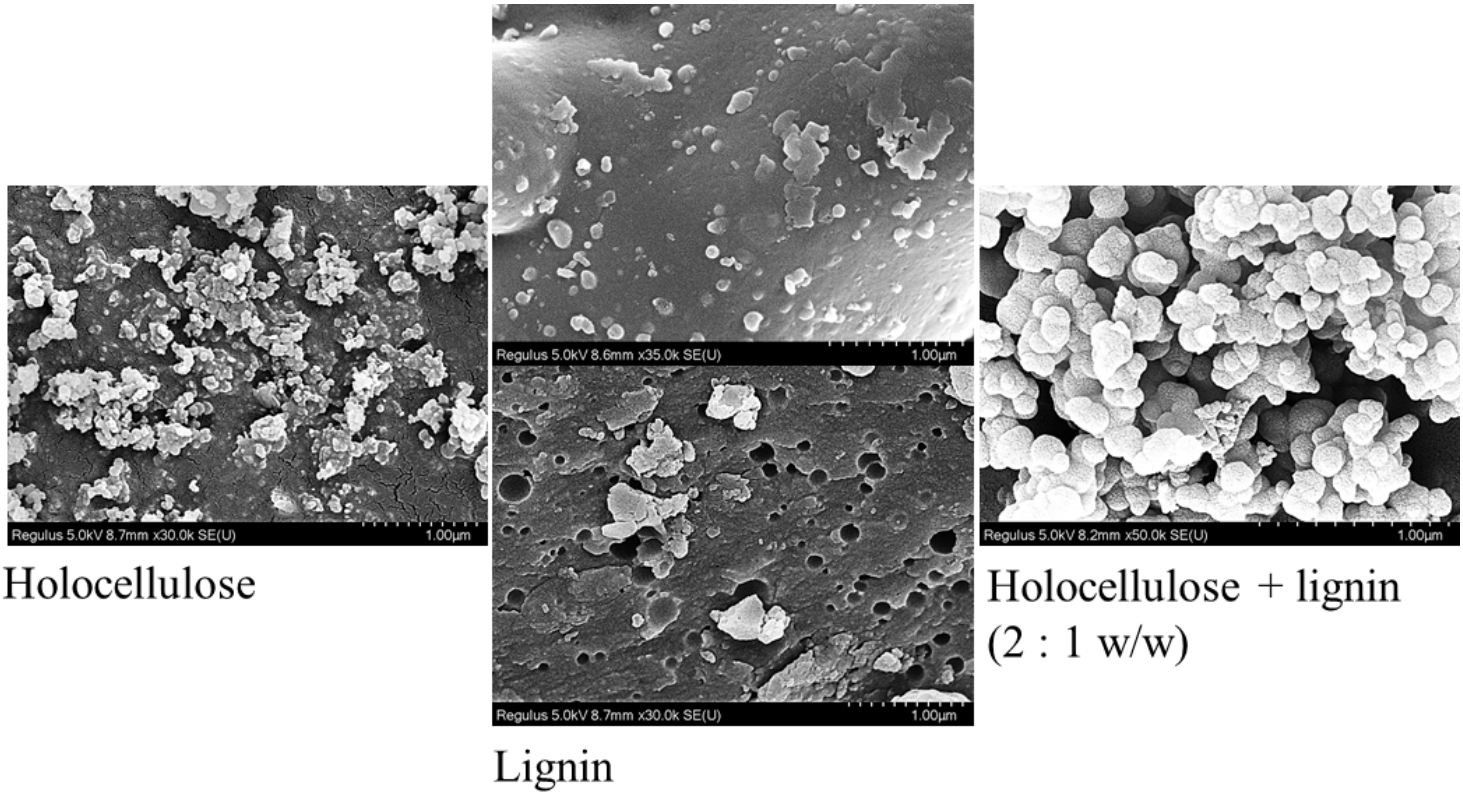

Figure 3

The morphology structure of acidic LiBr treated homocellulose (cellulose and hemicellulose), lignin, and homocellulose-lignin mixture (2:1 w/w).

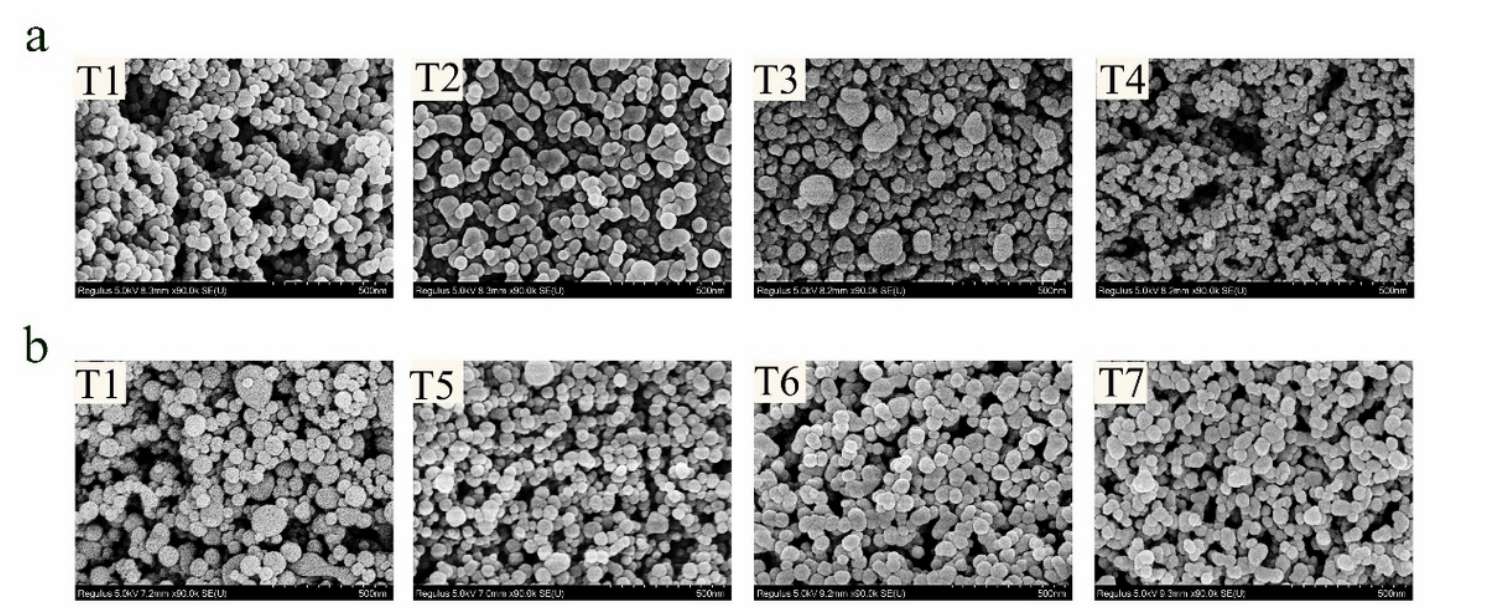

Figure 4

The morphology structure of biochar with different treatment conditions. a: the different temperature treatment with 0.5 M HCl respectively at 140 °C (T1), 160 °C (T2), 180 °C (T3), 200 °C (T4); b: the different

acid concentration at 140 °C with 0.5 M HCl (T1), 0.6 M HCl (T5), 0.8 M HCl (T6), 1.0 M HCl (T7).

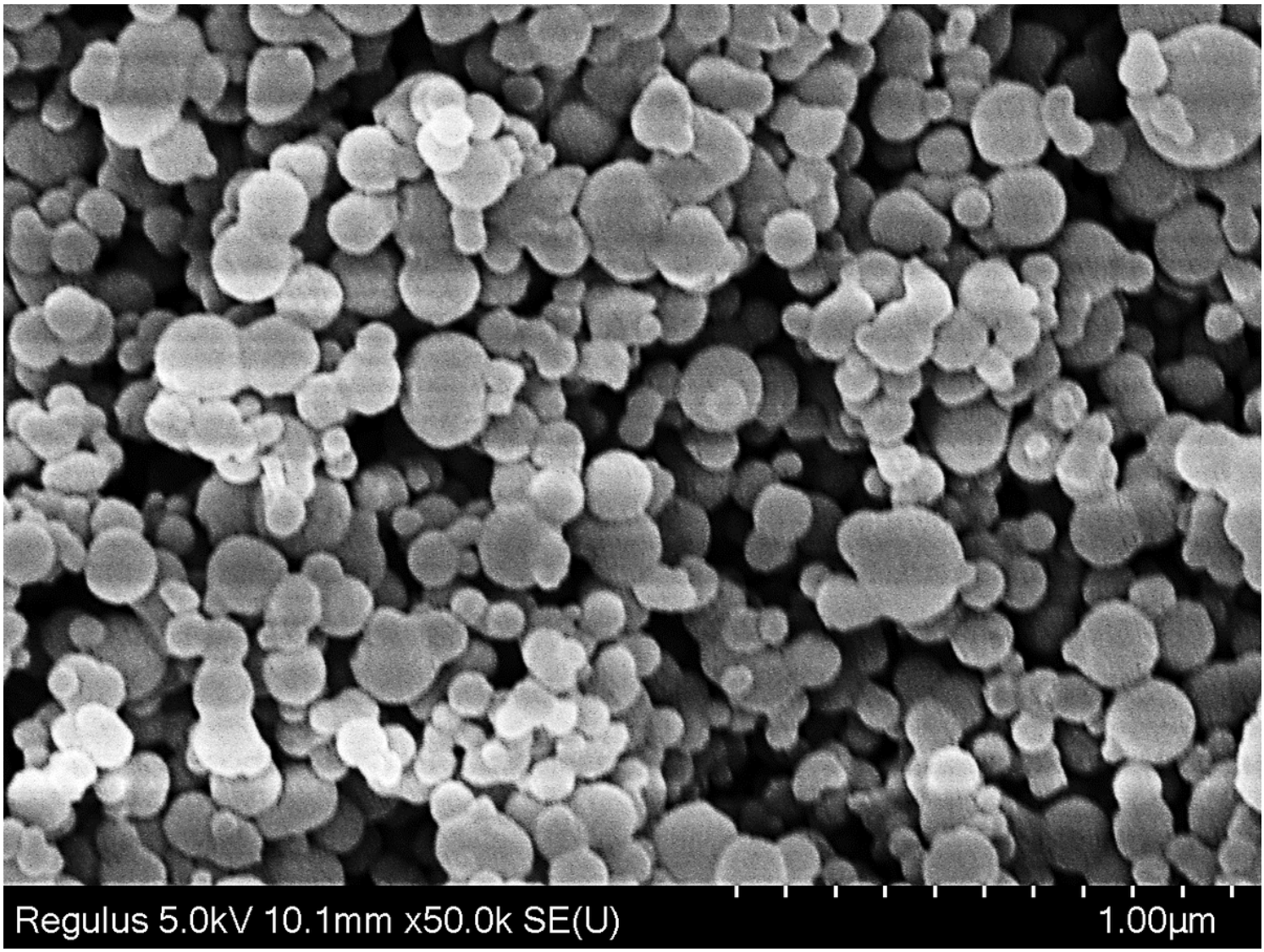

Figure 5

The morphology of biochar prepared from LiBr solution with fifth runs recycling

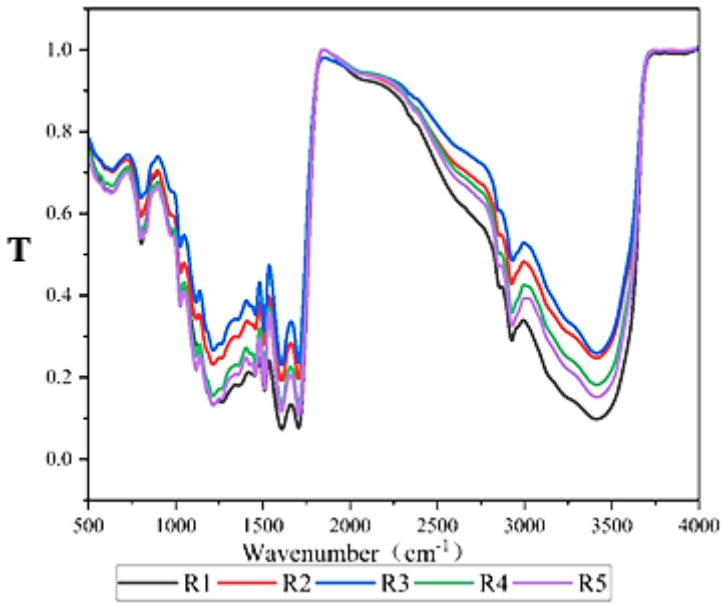

Figure 6

FTIR spectrum of the biochar from the recycling: the runs of recycles from run 1 to run 5 as R1 to R5.

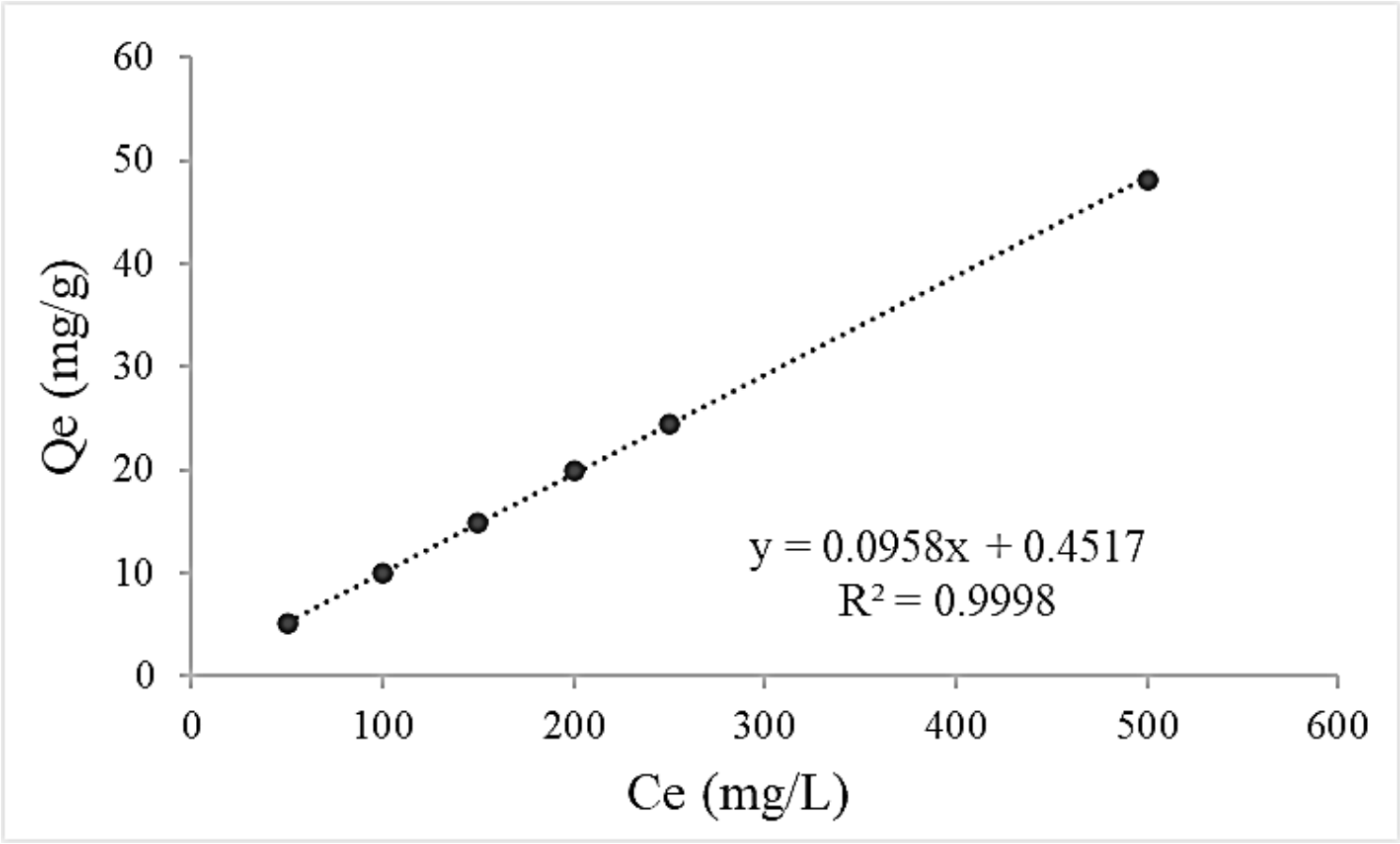

Figure 7

The removal capability of biochar to methyl orange, in which a well linear correlation was detected between the concentration of methyl orange and the adsorption capability of biochar (R2=0.9998).